

# Magnetic Relaxation in the Peak Effect Region of CeRu<sub>2</sub>\*

Pei-Chun Ho<sup>†</sup>, S. Moehlecke<sup>‡</sup> and M. B. Maple<sup>§</sup>  
 Institute for Pure and Applied Physical Sciences  
 and Department of Physics,  
 University of California, San Diego  
 La Jolla, CA 92093-0360, U.S.A.

November 5, 2018

## Abstract

The different pinning strengths of the flux line lattice in the peak effect (PE) region of a polycrystalline sample of CeRu<sub>2</sub> with a superconducting transition temperature  $T_c = 6.1$  K have been probed by means of magnetization measurements with a SQUID magnetometer as the temperature  $T$  and the magnetic field  $H$  are varied. Magnetic relaxation measurements were used to monitor the flux line dynamics in the PE region. For  $T < 4.5$  K and  $H < H_P$ , where  $H_P$  is the field where the magnetization reaches a maximum in the PE region, the relaxation rate was found to be significantly larger in the descending-field branch of the PE than it is in other sections of the PE region. For  $T \geq 4.5$  K, the relaxation rate in the entire PE region is so large that the magnetization reached a stable (equilibrium) value within  $10^4$  s. This experimentally determined stable state appears as an increase of the magnetization in the PE region and has a dome shape superimposed on a linear interpolation through the PE region. It was also found that the PE in CeRu<sub>2</sub> can be suppressed by rapid thermal cycling of the sample between 10 K and 300 K four times. The reversible magnetization after the PE has been suppressed coincides with the linear interpolation through the PE region, in contrast to the behavior of the equilibrium magnetization when the PE is present.

PACS number: 74.25.Qt, 74.70.Ad

## 1 Introduction

The peak effect (PE) has been observed in elements such as Nb, [1] heavy fermion compounds such as UPd<sub>2</sub>Al<sub>3</sub>, [2, 3] UPt<sub>3</sub>, [4] the low superconducting critical temperature ( $T_c$ ) C15 compound CeRu<sub>2</sub>, [5, 6] the layered compound NbSe<sub>2</sub>, [7, 8, 9, 10, 11, 12] the A15 compound V<sub>3</sub>Si, [13] and high  $T_c$  materials such as YBa<sub>2</sub>Cu<sub>3</sub>O<sub>7- $\delta$</sub> , [14] and Tl<sub>2</sub>Ba<sub>2</sub>CaCu<sub>2</sub>O<sub>8+ $\delta$</sub> . [15] This phenomenon occurs in type-II superconductors and is manifested as an increase of the critical current density (i.e., the irreversibility of the magnetization [16]) near the upper critical field  $H_{c2}$ . The PE originates from the softening of the flux line lattice (FLL) in the vicinity of  $H_{c2}$  where the fluxoids are more effectively pinned to randomly distributed pinning centers in a sample, such as defects, impurity atoms, grain boundaries, dislocations, etc. [17, 18] However, the PE is strongly material dependent, and the detailed understanding of this phenomenon is still lacking.

The cubic Laves-phase (C15) compound CeRu<sub>2</sub> exhibits superconductivity with a  $T_c \approx 6.1$  K, the highest value known for superconducting intermetallic compounds of Ce. It was speculated that the PE in CeRu<sub>2</sub> is caused by a first-order phase transition to the spatially nonuniform Fulde-Ferrel-Larkin-Ovchinnikov (FFLO) superconducting state, [19, 20, 21] which has also been

\*submitted to Phys. Rev. B

<sup>†</sup>email:pch@physics.ucsd.edu

<sup>‡</sup>Instituto de Física “Gleb Wataghin”, Universidade Estadual de Campinas, Unicamp, 13083-970, Campinas, São Paulo, Brasil. email:sergio@if.unicamp.br

<sup>§</sup>email:mbmaple@ucsd.edu

proposed to occur in the heavy fermion superconductors UPd<sub>2</sub>Al<sub>3</sub>, [2, 22] UBe<sub>13</sub>, [23] and UPt<sub>3</sub>. [4] Extensive transport, [5, 24] magnetostriction, [25] dc magnetization, [26, 27, 28, 9] ac magnetic susceptibility, [29, 9] and neutron scattering [30] measurements have been performed in the PE region of CeRu<sub>2</sub>. However, recent measurements of the mixed-state flux-flow resistivity [5, 24, 31] indicate that plastic deformation of the FLL may be responsible for CeRu<sub>2</sub>'s PE. In order to obtain more information about the flux line dynamics associated with the PE, we have performed measurements of the relaxation of the dc magnetization  $M$  as a function of temperature  $T$ , magnetic field  $H$  and time  $t$  in PE region for CeRu<sub>2</sub>.

## 2 Experimental Details

The as-cast large-grain polycrystalline CeRu<sub>2</sub> sample was produced by a Czochralski pulling method. [5] The sample has an irregular shape with dimensions  $\sim 2 \text{ mm} \times 1.5 \text{ mm} \times 1.5 \text{ mm}$ . An x-ray powder diffraction analysis confirmed that the CeRu<sub>2</sub> sample has the expected cubic C15 structure, although extra peaks due to Ru inclusions were also present.

The dc magnetization data were obtained with a MPMS-5.5 (Quantum Design, Inc.) superconducting quantum interference device (SQUID) magnetometer. After the sample was cooled in zero field (ZFC), the  $M(T)$  data yielded  $T_c = 6.1 \text{ K}$  with  $H = 100 \text{ Oe}$ . Special care was taken in the  $M(T, H, t)$  measurements in the PE region since it is known that the results of the measurements can be affected by the measuring process [32] that involves the movement of the sample in a magnetic field with small inhomogeneity. The magnetization measurements for several different scan lengths were tested, and a scan length of 1.5 cm was found to minimize the effect of the inhomogeneous field of the superconducting magnet without compromising significantly the signal sensitivity. The field inhomogeneity for such a scan length is  $\sim 0.004\%$ ; i.e.,  $\sim 1 \text{ Oe}$  for a field of 2 T. Each measurement consisted of an average over two scans ( $\sim 10 \text{ s/scan}$ ) in the fixed-range mode which prevented the performance of more than 2 scans in the measurements. The sample was observed to be paramagnetic in the normal state. Earlier resonant photoemission [33] and bremsstrahlung isochromat spectroscopy [34] studies of CeRu<sub>2</sub> have revealed a large amount of Ce 4f spectral weight in the vicinity of the Fermi level. Both the Ce 4f electrons and the excess Ru can contribute to the paramagnetic behavior of the CeRu<sub>2</sub> sample. The paramagnetic background of our sample was determined by measuring the magnetization  $M(H)$  above  $H_{c2}$  for each temperature.  $H_{c2}$  is defined as the field where  $M(H)$  starts to deviate from the linear paramagnetic behavior in the normal state. For the magnetization  $M$  data presented here, the linear paramagnetic background was removed and the data were normalized to the sample weight (47.62 mg).

The magnetization hysteresis loop in the PE region is composed of two branches: (1) the ascending-field branch where the flux lines are moving into the sample with increasing field, and (2) the descending-field branch where the flux lines are moving out of the sample with decreasing field. For a given temperature and field in the PE region, the relaxation of the magnetization was measured for both ascending- and descending-field branches. The measurements were performed as follows: In the ascending-field branch, the sample was ZFC from the normal state to the measuring temperature,  $T_M$ . The field was then raised in steps until it reached the measuring field,  $H_M$ . While  $H_M$  and  $T_M$  were held constant, the magnetization was measured as a function of time. For the descending-field branch, the field was either increased to  $\sim 2 \text{ T}$  above  $H_{c2}$  at  $T_M$  or the sample was FC (field cooled) from 10K to  $T_M$  at  $H \geq H_{c2}(T_M)$  to ensure the full flux penetration (i.e., the descending-field branch always started from the normal state of CeRu<sub>2</sub>). The field was then lowered by steps to  $H_M$  to measure the relaxation of the magnetization. Because the PE region is strongly history-dependent, the field steps for increasing and decreasing the field were kept the same to maintain the same initial conditions for each relaxation measurement. Between each pair of relaxation measurements (ascending and descending branches with the same  $T$ ), the temperature of the sample was raised to 10 K ( $> T_c$ ) and the remanent field of the magnet was minimized by oscillating the field from 2 T to 0 T.

### 3 Results

The magnetic field dependencies of the magnetization  $M(H)$  in CeRu<sub>2</sub>'s PE region for various temperatures between 2 K and 5 K are shown in Fig. 1. The irreversible peak feature in  $M(H)$  appears between  $H_{irr-}$  and  $H_{irr+}$ , the low and high fields where magnetization hysteresis occurs. However, when  $T < 4.2$  K,  $H_{irr-}$  appears in different fields for the ascending- and descending-field branches (defined as  $H_{irr-asc}$  and  $H_{irr-desc}$ , respectively). With increasing magnetic field, the PE starts at  $H_{irr-asc}$ , whereas with decreasing field from above  $H_{c2}$ , the magnetization hysteresis persists down to  $H_{irr-desc} < H_{irr-asc}$ . This difference in  $H_{irr-asc}$  and  $H_{irr-desc}$  is not observed in the magnetization data  $M(H)$  above 4.5 K due to the fast relaxation rates at these temperatures as we will show later. As for  $H_{irr+}$ , there is no difference in this quantity between the two branches. The location of the PE region and  $H_{c2}$  are displayed in the  $H - T$  phase diagram in the inset of Fig. 1. As  $T$  increases, the height and width of the hysteresis in  $M(H)$  gradually decrease. The PE becomes undetectable within the resolution of the MPMS for  $T > 4.7$  K. For each PE hysteresis loop, the beginning of the irreversibility corresponds to an increase in the critical current density  $J_c \propto \Delta M (\equiv M_{desc}(H) - M_{asc}(H))$  where  $M_{asc/desc}$  is the magnetization from the ascending/descending-field branch) which is a result of the increase of the effective pinning strength of the FLL. After the field passes through  $H_P$  (the field where the maximum magnetization hysteresis occurs within the PE region), the subsequent reduction in size of the hysteresis loop of the PE corresponds to a decrease of the FLL pinning, yielding a reduction in  $J_c$ .

The measurements of the isothermal relaxation of the magnetization of CeRu<sub>2</sub> were performed at constant fields within the PE region for  $T$  between 2 K and 5 K. Shown in Figs. 2 and 3 are the raw magnetization relaxation data  $M(H, t)$  for six different fields at 4.2 K and 4.5 K, respectively. The top panels in Figs. 2 and 3 show the evolution of the magnetization with time in the  $M - H$  plane, and panels (a)-(f) depict the time dependence of the magnetization  $M(t)$  after a specified  $H$  was reached in both branches at 4.2 K and 4.5 K. At 4.2 K and 2.01 T, the relaxation rate ( $|dM/d(\ln t)|$ ) in the descending-field branch changes from  $\sim 3.34 \times 10^{-2}$  to  $\sim 2.32 \times 10^{-4}$  after 300 s; the ascending- and descending-field magnetization after 300 s merges to the same value (Fig. 2(a)). At a different  $H$  of 2.025 T (Fig. 2(b)) (closer to  $H_P = 2.05$  T), the descending-field relaxation rate changes from  $\sim 3.23 \times 10^{-2}$  to  $\sim 2.16 \times 10^{-3}$  after 1000 s and the ascending-field rate after 500 s is  $\sim 1.46 \times 10^{-3}$ . The magnetizations in each branch nearly merged to a stable value within  $10^4$  s. For  $H \geq H_P$ , the magnetization in each branch depends approximately linearly on the logarithm of time. However, the magnetization in these fields cannot reach a stable value within  $\sim 10^4$  s. From the intersection of two straight lines that were fitted to the  $M(\ln t)$  data, the time of  $\sim 2 \times 10^6$  s was estimated for the magnetization to reach a stable value in the PE region  $H \geq H_P$  at 4.2 K. Thus, at 4.2 K in the PE region, for  $H < H_P$ , the relaxation in the descending-field branch is dramatically faster than it is in the ascending-field branch. Compared to 4.2 K data, the relaxation at 4.5 K is even faster. The 4.5 K magnetizations from each branch can merge to a stable value within 3000 s across the entire PE region (Fig. 3).

Because  $J_c \propto \Delta M$ , the flux pinning force density  $F_p = J_c \times B/c$  and  $B \sim H$ , it follows that  $F_p \propto \Delta M \times H$ . Fig. 4 illustrates the normalized effective pinning force  $f_p$  as a function of time at 3 K in (a) and 4.2 K in (b) where  $f_p$  is defined as  $(\Delta M / \Delta M_{max-init}) \times (H/H_{c2})$  and  $\Delta M_{max-init}$  is the initial size of  $\Delta M$  at  $H_P$ . As the magnetic field approaches  $H_P$ ,  $f_p$  becomes stronger and reaches a maximum at  $H_P$ . Although the initial value of  $f_p$  is the same for two different values of  $H$  above and below  $H_P$ ,  $f_p$  for  $H < H_P$  relaxes much faster than  $f_p$  for  $H > H_P$ . Hence,  $H \geq H_P$  is a stronger pinning region of the PE, and  $f_p$  has more linear logarithmic time dependence here. The  $H \geq H_P$  data at 3 K can be well represented by expression for  $f_p$  from the Anderson-Kim thermally activated flux creep model,  $f_p \propto [1 - (k_B T/U_0) \ln t]$  where  $k_B$  is Boltzmann's constant. [35, 36, 37, 38] The activation energy  $U_0$  for fluxoid depinning is estimated to be  $\sim 115$  K. For  $T = 4.2$  K and  $H > H_P$ , the relaxation deviates from the linear logarithmic time dependence and  $f_p$  can be described with the collective flux creep model [39] which yields  $f_p \propto 1/[1 - (\mu k_B T/U_0) \ln(t/t_0)]^{(1/\mu)}$  where  $t_0$  is a macroscopic quantity depending on the sample size and  $\mu$  comes from  $U(J) \propto J^{-\mu}$ . For  $H = 2.085$

T, 2.105 T, and 2.135 T,  $\mu \sim 0.48, 0.73,$  and  $0.78,$  respectively, which are reasonable values as expected from the collective creep model. The relaxation data for  $H < H_P$  at both  $T = 3$  K and 4 K, the relaxation data cannot be described by any known model.

Fig. 5 shows the time evolution of magnetization hysteresis loops  $M(H)$  of the PE at 3 K, 4.2 K, and 4.5 K. The dotted line connects the final values of the magnetization at the end of the relaxation measurements at each temperature (i.e.,  $\sim 10^4$  s after the initial state). For  $T \leq 4.2$  K, the hysteresis loops of the PE evolve toward smaller loops, but for  $T \geq 4.5$  K, the hysteresis loops disappear after  $\sim 3000$  s and the magnetization from both branches reaches a stable value within the PE region.

Since for  $T \geq 4.5$  K the magnetization from both branches reaches about the same value after  $\sim 3000$  s, a stable value of the magnetization of CeRu<sub>2</sub> at each field can be determined by averaging the last 300 s of magnetization data  $M(t)$  at 4.5 and 4.7 K. Fig. 6 depicts the experimentally determined stable state of the magnetization of CeRu<sub>2</sub> ( $M_{stable}$ ) within the PE. This experimentally determined  $M_{stable}$  is dome-shaped with a maximum slightly above  $H_P$ . However, we also found the PE of CeRu<sub>2</sub> at 4.5 K can be suppressed by rapid thermal cycling of the sample between 10 K and 300 K several times. After the PE is destroyed at 4.5 K, the magnetization becomes reversible and follows approximately the linear interpolation between the beginning and the end of the initial hysteresis loop of the PE (Fig. 7).

## 4 Discussion

Previous measurements [5, 24, 31] of the flux flow resistance  $R(H)$  in the mixed state of CeRu<sub>2</sub> showed field hysteresis at the lower onset of the PE region: for  $J < J_c$ , near the onset of the PE the resistance is higher in the ascending field branch than in the descending-field branch. The flux motion is inhibited more in the descending-field branch near the lower onset of the PE. This behavior is equivalent to the observed mismatch  $H_{irr-desc} < H_{irr-asc}$  in the  $M(H)$  data for  $T \leq 4.2$  K (Fig. 1), except at the same temperature it is more pronounced in resistivity data than the magnetization data. [5] This hysteresis at the lower onset of the PE was also observed in several superconducting materials, such as 2H-NbSe<sub>2</sub>, [9, 40] Ca<sub>3</sub>Rh<sub>4</sub>Sn<sub>13</sub>, [41] and Nb. [42] Also shown by the relaxation data of the magnetization (Fig. 2), the flow of the FLL in this portion of the PE changes very quickly from the behavior of a softer FLL (i.e., larger pinning) in the beginning to more coherent motion of a stiff FLL (i.e., reduction of pinning). Thus, this hysteresis seems strongly connected to the metastable disordered phase generated by edge contamination observed in 2H-NbSe<sub>2</sub>. [10, 11, 12]. Furthermore, it is believed that bulk pinning is greatly reduced in more 2-dimensional compound 2H-NbSe<sub>2</sub>. [12] However, the similarity of behavior of the fluxoids in the PE region of the cubic CeRu<sub>2</sub> compound to that of NbSe<sub>2</sub> indicates that the underlying pinning mechanism may be independent of crystal dimensionality.

As observed from the relaxation data, the FLL in the disordered state for  $T < 4.5$  K and  $H > H_P$  has not yet reached a thermal equilibrium state since its effective pinning force is still decreasing towards zero. As  $T \geq 4.5$  K, vortex lines can reach an equilibrium state by fast relaxation that is possibly due to thermal fluctuations or to the shaking effect [43, 11] caused by the scanning movement of the sample from one pick up coil to the other in SQUID magnetometer. The stable-state magnetization (Fig. 6) we determined from magnetic relaxation in the PE of CeRu<sub>2</sub> is reminiscent of a phase transition, especially compared with the magnetization data taken in the same sample after its PE is suppressed (Fig. 7). Recently, two experiments were reported in which the stable-state magnetization of CeRu<sub>2</sub> in the PE region was determined by cycling the magnetic field with a small amplitude at 4.5 K in CeRu<sub>2</sub>'s PE. [27, 28] The stable-state magnetization derived from our relaxation measurements is straightforward and does not depend by any model, [44] in contrast to the magnetic-field-cycling experiments. The stable-state magnetization determined by Roy et al. [27] has the same dome shape as found in our equilibrium magnetization, but the magnetization found by Tulapurkar et al. [28] has a step shape. Although these experimental results do not agree with one another, in both cases this stable state was considered to result from

an occurrence of a first order phase transition.

If the stable-state magnetization at 4.5 K and 4.7 K is assumed to be related to the first order melting of the FLL, then the jump in magnetization expected for such a vortex melting transition can be estimated from the Clausius-Claperon relation,  $\Delta S = -\Delta M_{melting} dH_m/dT$ . [45] The entropy change at the transition per unit volume is  $\Delta S \approx c_L^2 C_{66}/T_m$ , [46] where  $c_L \approx 0.2$  is the Lindemann number and  $C_{66} \approx [BH_{c1}/(16\pi)](1-b)^2$  is the vortex-lattice shear modulus for an isotropic superconductor [38] where  $b \equiv B/H_{c2}$ . At  $T_m = 4.5$  K,  $B \sim H_P = 17.55$  kOe,  $H_{c1} \sim 300$  Oe and  $H_{c2} \sim 19.8$  kOe, this gives  $C_{66} \approx 1353$  erg/cm<sup>3</sup> and  $\Delta S \approx 12.03$  erg/K-cm<sup>3</sup>. From  $M_{stable}(H)$  data at 4.5 K and 4.7 K (Fig. 6),  $dH_m/dT$  is assumed to be the same as  $dH_P/dT \approx -10.75$  kOe/K and  $\Delta M_{melting}$  is estimated to be  $1.12 \times 10^{-3}$  emu/cm<sup>3</sup>; i.e.,  $1.05 \times 10^{-4}$  emu/g where the density [25] of CeRu<sub>2</sub> is 10.62 g/cm<sup>3</sup>. This estimate of  $\Delta M_{melting}$  is much smaller than what we observed from  $\Delta M \sim 1 \times 10^{-2}$  emu/g at 4.5 K and  $\sim 4 \times 10^{-3}$  emu/g at 4.7 K (Fig. 6). Whether the stable-state magnetization is associated with a first order melting in the the PE region but is obscured by the disordered phase appearing near the sample surface, the magnetization data alone are not sufficient for resolving this issue. Thus, whether the FLL undergoes a first-order or continuous phase transition in the PE region or simply just a crossover of the dynamical behavior is not yet clear.

How CeRu<sub>2</sub>'s PE can be suppressed by rapid thermal cycling of the temperature between 10 K and 300 K is still a mystery. Previous low temperature X-ray diffraction studies show the Laves phase compounds LaRu<sub>2</sub> [47] and (La<sub>1-x</sub>,Ce<sub>x</sub>)Ru<sub>2</sub> [48] with  $x < 0.25$  undergo a cubic-tetragonal structural transition at  $\sim 30$  K. We suspected a small part of the CeRu<sub>2</sub> sample might also undergo a similar structural phase transition at some temperature between 10 K and 300 K. Small regions of transformed structure within the sample could provide pinning centers. If the sample temperature was changed rapidly, the high temperature Laves phase crystal structure of CeRu<sub>2</sub> might be quenched to low temperature and reduce the PE. However, the previous X-ray studies did not provide any evidence of such a structural phase transformation in CeRu<sub>2</sub> [48]. After suppressing the PE, we also thermally cycled the sample at a rate of 10 K/min to test whether some significant change in magnetization in the PE region at certain temperature between 10 K and 300K would occur in support of our hypothesis. However, this experiment did not yield conclusive results.

## 5 Summary

In summary, we have performed magnetic relaxation measurements between 2 K and 4.7 K in the PE region of CeRu<sub>2</sub>. For  $T \leq 4.2$  K, due to stronger pinning, the FLL relaxes at a much slower rate and does not reach a stable state within the duration of the measurement ( $\sim 1.2 \times 10^4$  s). The dynamics of the FLL for  $H < H_P$  in the descending-field branch are very different than in the other parts of the PE region, and the pinning strength is stronger for  $H > H_P$  than for  $H < H_P$ . For  $T \geq 4.5$  K, a stable-state magnetization exists across the PE region that has a dome shape with a maximum occurring slightly above  $H_P$  and agrees with the result of magnetic-field-cycling measurements by Roy et al. [27] We also found that the PE of CeRu<sub>2</sub> can be removed by rapid thermal cycling of the sample between room temperature and 10 K several times, and the reversible magnetization follows a linear interpolation across the PE region. Compared with the reversible magnetization of CeRu<sub>2</sub> without the PE, the stable-state magnetization associated with the appearance of the PE is reminiscent of a phase transition. However, the size of the stable-state magnetization jump at  $H_P$  is much larger than expected for a first order melting of the FLL. Whether this stable-state magnetization is related to a first-order or a continuous phase transition, or simply a dynamical crossover of the FLL is not yet clear.

## 6 Acknowledgement

We thank Professor Daniel Arovas for helpful discussions. This research was supported by the U. S. Department of Energy under Grant No. DEFG-03-86ER-45230.

## References

- [1] S. H. Autler, E. S. Rosenblum, and K. H. Gooen, Phys. Rev. Lett. **9**, 489 (1962).
- [2] K. Gloos, R. Modler, H. Schimanski, C. D. Bredl, C. Geibel, F. Steglich, A. I. Buzdin, N. Sato, and T. Komatsubara, Phys. Rev. Lett. **70**, 501 (1993).
- [3] A. Ishiguro, A. Sawada, Y. Inada, J. Kimura, M. Suzuki, N. Sato, and T. Komatsubara, J. Phys. Soc. Jpn. **64**, 378 (1995).
- [4] K. Tenya, M. Ikeda, T. Tayama, H. Mitamura, H. Amitsuka, T. Sakakibara, K. Maezawa, N. Kimura, R. Settai, and Y. Onuki, J. Phys. Soc. Jpn. **64**, 1063 (1995).
- [5] N. R. Dilley, J. Herrmann, S. H. Han, M. B. Maple, S. Spagna, J. Diederichs, and R. E. Sager, Physica C **265**, 150 (1996).
- [6] N. R. Dilley and M. B. Maple, Physica C **278**, 207 (1997).
- [7] S. Bhattacharya and M. J. Higgins, Phys. Rev. Lett. **70**, 2617 (1993).
- [8] W. Henderson, E. Y. Andrei, M. J. Higgins, and S. Bhattacharya, Phys. Rev. Lett. **77**, 2077 (1996).
- [9] S. S. Banerjee, N. G. Patil, S. Saha, S. Ramakrishnan, A. K. Grover, S. Bhattacharya, G. Ravikumar, P. K. Mishra, T. V. Chandrasekhar Rao, V. C. Sahni, M. J. Higgins, E. Yamamoto, Y. Haga, M. Hedo, Y. Inada, and Y. Onuki, Phys. Rev. B **58**, 995 (1998).
- [10] Y. Paltiel, E. Zeldov, Y. N. Myasoedov, H. Shtrikman, S. Bhattacharya, M. J. Higgins, Z. L. Xia, E. Y. Andrei, P. Gammel, and D. J. Bishop, Nature **403**, 398 (2000).
- [11] Y. Paltiel, E. Zeldov, Y. Myasoedov, M. L. Rappaport, G. Jung, S. Bhattacharya, M. J. Higgins, Z. L. Xia, E. Y. Andrei, P. L. Gammel, and D. J. Bishop, Phys. Rev. Lett. **85**, 3712 (2000).
- [12] Y. Paltiel, D. T. Fuchs, E. Zeldov, Y. N. Myasoedov, H. Shtrikman, M. L. Rappaport, and E. Y. Andrei, Phys. Rev. B **58**, R14763 (1998).
- [13] M. Isino, T. Kobayashi, N. Toyota, T. Fukase, and Y. Muto, Phys. Rev. B **38**, 4457 (1988).
- [14] W. K. Kwok, J. A. Fendrich, C. J. van der Beek, and G. W. Crabtree, Phys. Rev. Lett. **73**, 2614 (1994).
- [15] V. Hardy, A. Wahl, A. Ruyter, A. Maignan, C. Martin, L. Coudrier, J. Provost, and C. Simon, Physica C **232**, 347 (1994).
- [16] W. A. Fietz and W. W. Web, Phys. Rev. **178**, 657 (1969).
- [17] A. B. Pippard, Philosophical magazine **19**, 217 (1969).
- [18] A. I. Larkin and Y. N. Ovchinnikov, J. Low Temp. Phys. **34**, 409 (1979).
- [19] P. Fulde and R. A. Ferrell, Phys. Rev. **135**, A 550 (1964).
- [20] A. I. Larkin and Y. N. Ovchinnikov, Sov. Phys. JETP **20**, 762 (1965).
- [21] L. W. Grunenberg and L. Gunther, Phys. Rev. Lett. **16**, 996 (1966).
- [22] F. Steglich, C. Geibel, K. Gloos, P. Hellmann, R. Kohler, M. Lang, R. Modler, and C. Schank, Physica C **235-240**, 95 (1994).

- [23] F. Thomas, B. Wand, T. Luhmann, P. Gegenwart, G. R. Stewart, F. Steglich, J. P. Brison, A. Buzdin, L. Glemot, and J. Flouquet, *J. Low Temp. Phys.* **102**, 117 (1996).
- [24] H. Sato, Y. Kobayashi, H. Sugawara, Y. Aoki, R. Settai, and Y. Onuki, *J. Phys. Soc. Jpn.* **65**, 1536 (1996).
- [25] R. Modler, P. Gegenwart, M. Lang, M. Deppe, M. Weiden, T. Luhmann, C. Geibel, F. Steglich, C. Paulsen, J. L. Tholence, N. Sato, T. Komatsubara, Y. Onuki, M. Tachiki, and S. Takahashi, *Phys. Rev. Lett.* **76**, 1292 (1996).
- [26] G. W. Crabtree, M. B. Maple, W. K. Kwok, J. Herrmann, J. A. Fendrich, N. R. Dilley, and S. H. Han, *Physics Essays* **9**, 628 (1996).
- [27] S. B. Roy, P. Chaddah, and L. E. DeLong, *Physica C* **304**, 43 (1998).
- [28] A. A. Tulapurkar, D. Heidarian, S. Sarkar, S. Ramakrishnan, A. K. Grover, E. Yamamoto, Y. Haga, M. Hedo, Y. Inada, and Y. Onuki, *Physica C* **355**, 59 (2001).
- [29] T. Nakama, M. Hedo, T. Maekawa, M. Higa, R. Resel, H. Sugawara, R. Settai, Y. Onuki, and K. Yagasaki, *J. Phys. Soc. Jpn.* **64**, 1471 (1995).
- [30] A. Huxley, R. Cubitt, D. McPaul, E. Forgan, M. Nutely, H. Mook, M. Yethiraj, P. Lejay, D. Caplan, and M. J. Penisson, *Physica B* **223-224**, 169 (1996).
- [31] N. R. Dilley, J. Herrmann, S. H. Han, and M. B. Maple, *Phys. Rev. B* **56**, 2379 (1997).
- [32] G. Ravikumar, T. V. Chandrasekhar, P. K. Mishra, V. C. Sahni, S. Saha, S. S. Banerjee, N. G. Patil, A. K. Grover, S. Ramakrishnan, S. Bhattacharya, E. Yamamoto, Y. Haga, M. Hedo, Y. Inada, and Y. Onuki, *Physica C* **276**, 9 (1997).
- [33] J. W. Allen, S.-J. Oh, I. Lindau, M. B. Maple, J. F. Suassuna, and S. B. Hagstrom, *Phys. Rev. B* **26**, 445 (1982).
- [34] J. W. Allen, S.-J. Oh, M. B. Maple, and M. S. Torikachvili, *Phys. Rev. B* **28**, 5347 (1983).
- [35] P. Anderson, *Phys. Rev. Lett.* **9**, 309 (1962).
- [36] Y. B. Kim, C. F. Hampstead, and A. R. Strnad, *Phys. Rev. Lett.* **9**, 306 (1962).
- [37] P. W. Anderson and Y. B. Kim, *Rev. Mod. Phys.* **36**, 39 (1964).
- [38] M. Tinkham, *Introduction to superconductivity* (McGraw-Hill, Inc., New York, 1996).
- [39] M. V. Feigel'man, V. B. Geshkenbein, A. I. Larkin, and V. M. Vinokur, *Phys. Rev. Lett.* **63**, 2303 (1989).
- [40] G. Ravikumar, P. K. Mishra, V. C. Sahni, S. S. Banerjee, A. K. Grover, S. Ramakrishnan, P. L. Gammel, D. J. Bishop, E. Bucher, M. J. Higgins, and S. Bhattacharya, *Phys. Rev. B* **61**, 12490 (2000).
- [41] S. Sarkar, D. Pal, S. S. Banerjee, S. Ramakrishnan, A. K. Grover, C. V. Tomy, G. Ravikumar, P. K. Mishra, V. C. Sahni, G. Balakrishnan, D. McK. Paul, and S. Bhattacharya, *Phys. Rev. B* **61**, 12394 (2000).
- [42] Y. Kopelevich and S. Moehlecke, *Phys. Rev. B* **58**, 2834 (1998).
- [43] T. Giamarchi and P. Le Doussal, *Phys. Rev. Lett.* **76**, 3408 (1996).
- [44] G. Ravikumar, K. V. Bhagwat, V. C. Sahni, A. K. Grover, S. Ramakrishnan, and S. Bhattacharya, *Phys. Rev. B* **61**, R6479 (2000).

- [45] A. Schilling, R. A. Fisher, N. E. Phillips, U. Welp, D. Dasgupta, W. K. Kwok, and G. W. Crabtree, *Nature* **382**, 791 (1996).
- [46] E. Zeldov, D. Majer, M. Konczykowski, V. B. Geshkenbein, V. M. Vinokur, and H. Shtrikman, *Nature* **375**, 373 (1995).
- [47] A. C. Lawson, K. Babershke, and E. U., *Phys. Lett.* **48A**, 107 (1974).
- [48] R. N. Shelton, A. C. Lawson, and K. Babershke, *S. S. Comm.* **24**, 465 (1977).

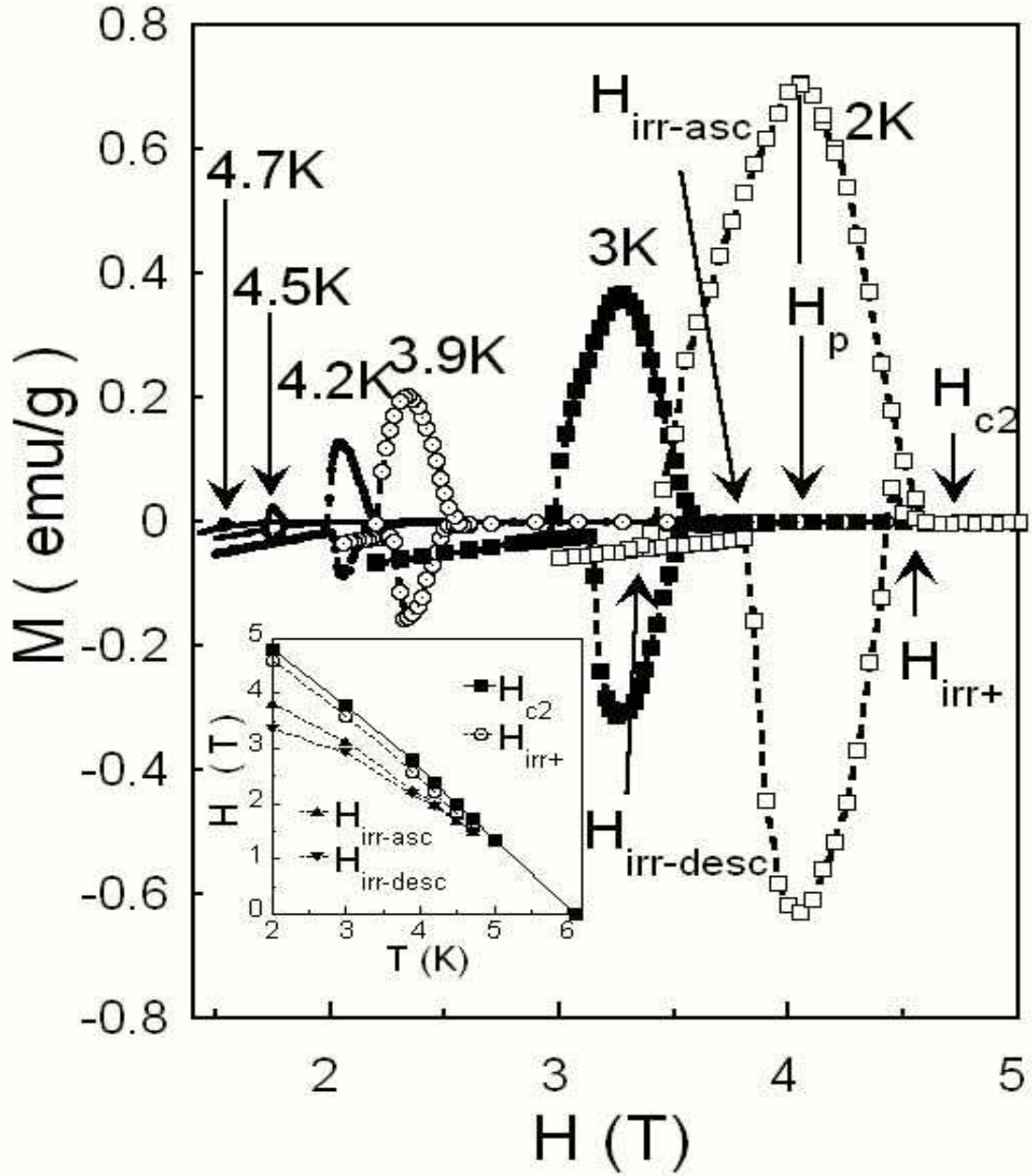


Figure 1: A set of hysteresis loops in dc magnetization  $M(H)$  of polycrystalline CeRu<sub>2</sub> in the PE region between 2 K and 4.7 K. Inset:  $H - T$  diagram of CeRu<sub>2</sub>.  $H_{irr+}$  is defined as the field where PE disappears,  $H_{irr-asc}$  as the onset field in the ascending-field branch,  $H_{irr-desc}$  as the onset field in the descending-field branch, and  $H_p$  as the field where the maximum of the irreversible magnetization occurs. The mismatch between  $H_{irr-asc}$  and  $H_{irr-desc}$  becomes more pronounced with decreasing temperatures.

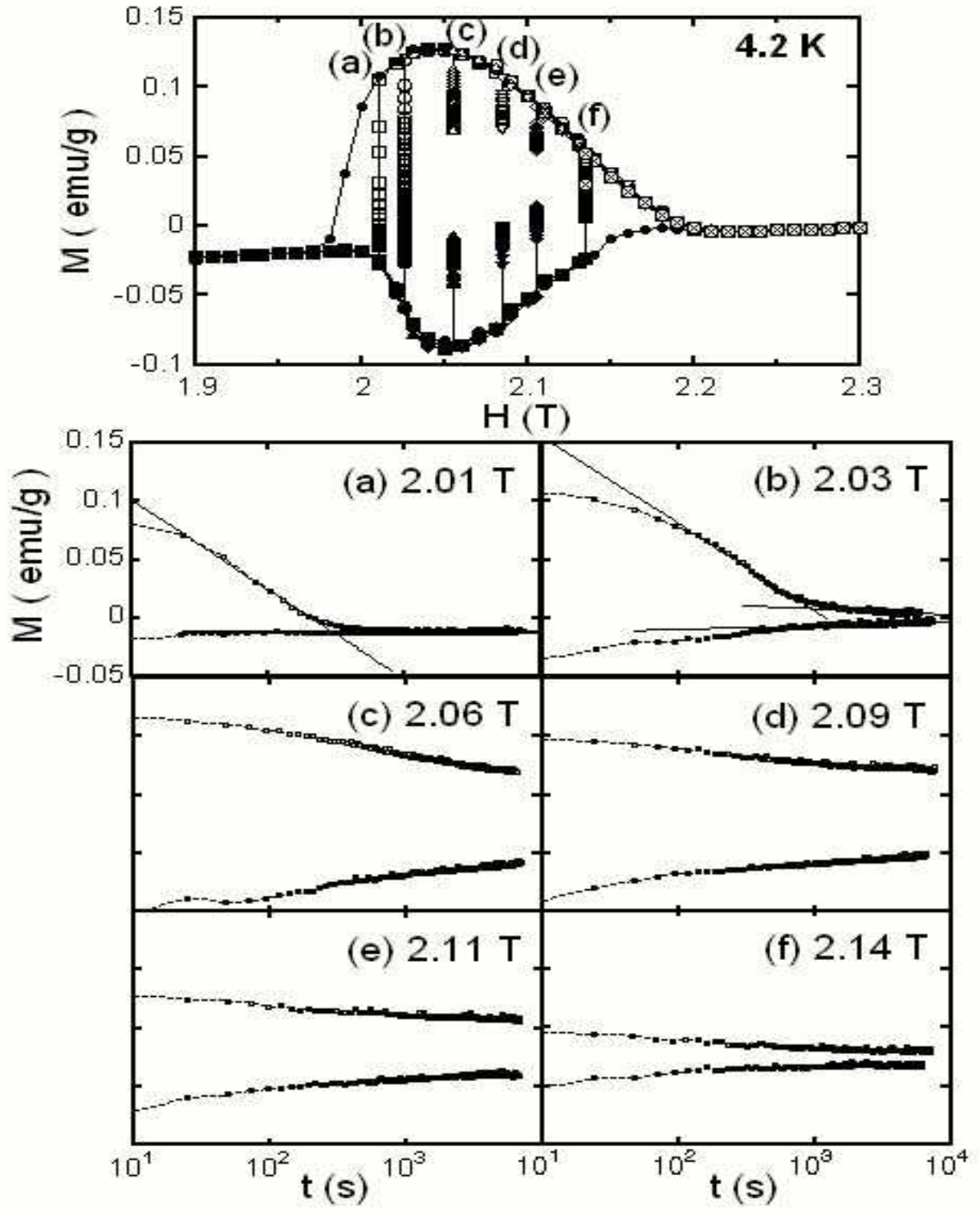


Figure 2: Relaxation of the magnetization  $M$  of  $\text{CeRu}_2$  at six different fields  $H$  in the PE region at 4.2 K.  $M$  is plotted vs  $H$  in the top panel. Panels (a)-(f) show  $M$  vs  $t$  at each  $H$  and all have the same vertical and horizontal scales. The bottom curve is from the ascending-field branch, and the top curve is from the descending-field branch. The slopes ( $dM(\text{emu/g})/d(\ln t)$ ) of the straight lines are: panel(a),  $\sim -3.34 \times 10^{-2}$  and  $\sim 2.15 \times 10^{-4}$ ; panel(b),  $\sim -3.32 \times 10^{-2}$ ,  $\sim -2.16 \times 10^{-3}$ , and  $\sim 1.46 \times 10^{-3}$ .

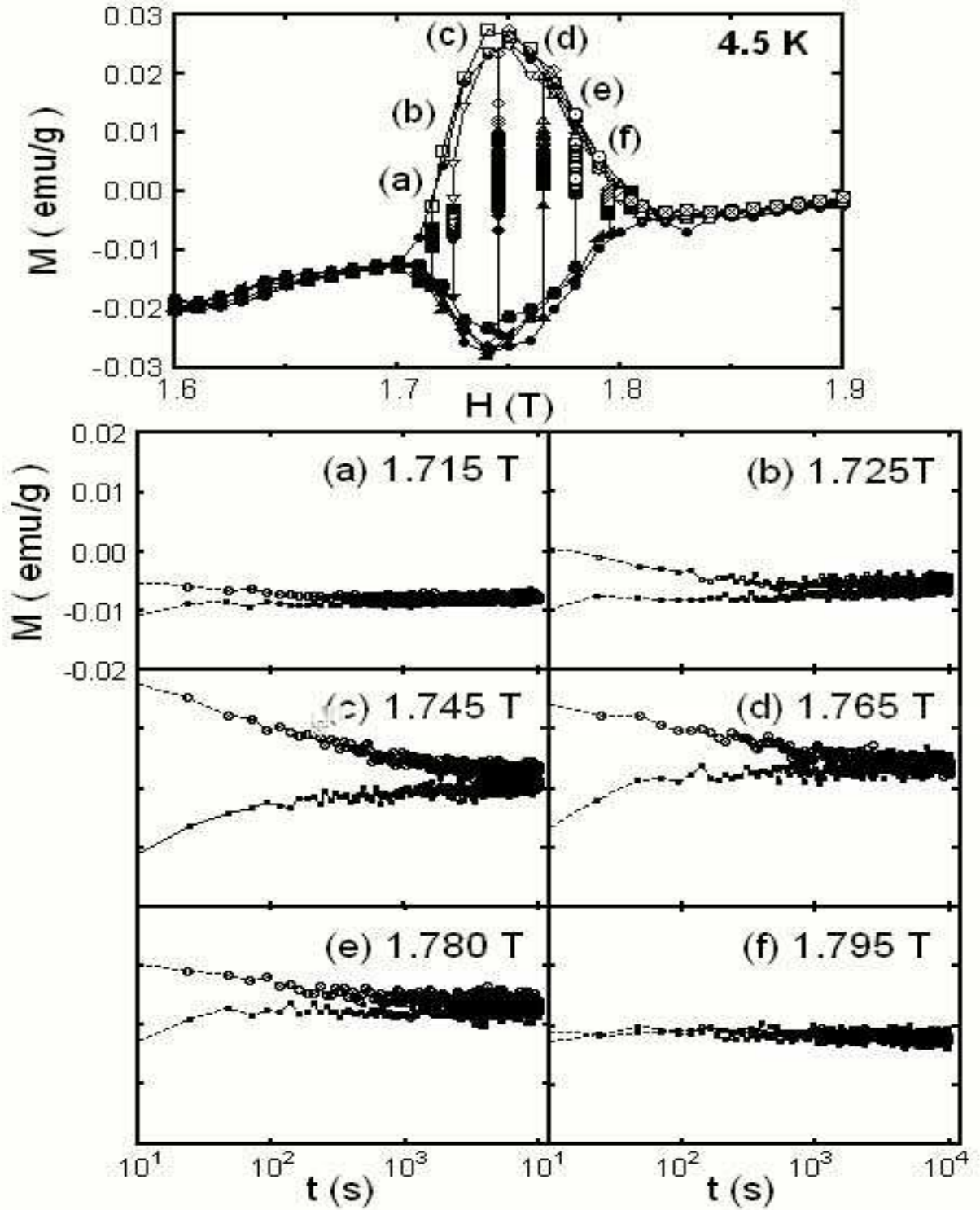


Figure 3: Relaxation of the magnetization  $M$  of  $\text{CeRu}_2$  at six different magnetic fields in the PE region at 4.5 K. The  $M$  is plotted vs  $H$  in the top panel. Panels (a)-(f) show  $M$  vs  $t$  at each  $H$  and all have the same vertical and horizontal scales. The bottom curve is from the ascending-field branch, and the top curve is from the descending-field branch.

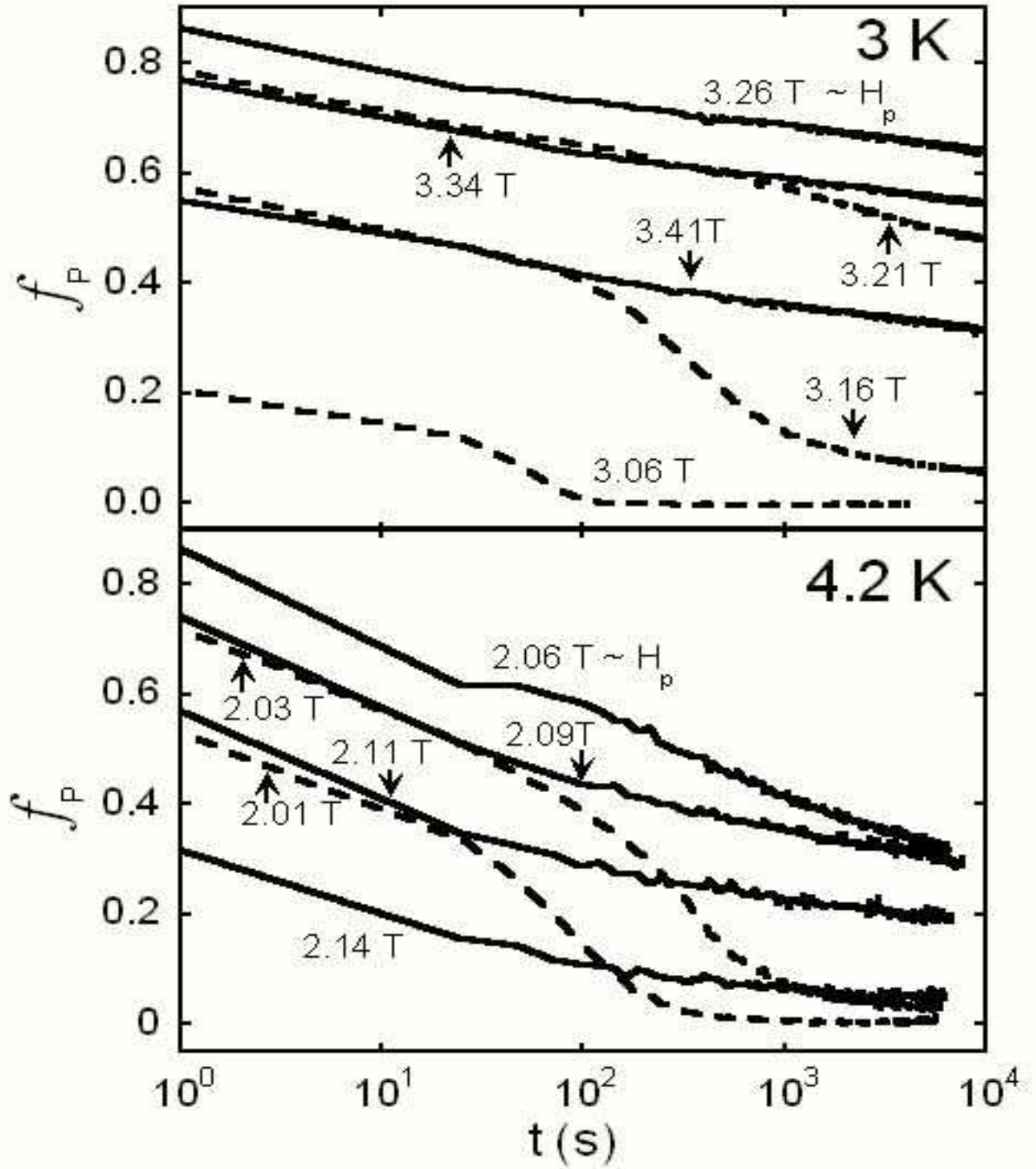


Figure 4: Time dependence of the normalized pinning force  $f_p$  at six different fields for 3 K and 4.2 K, respectively.

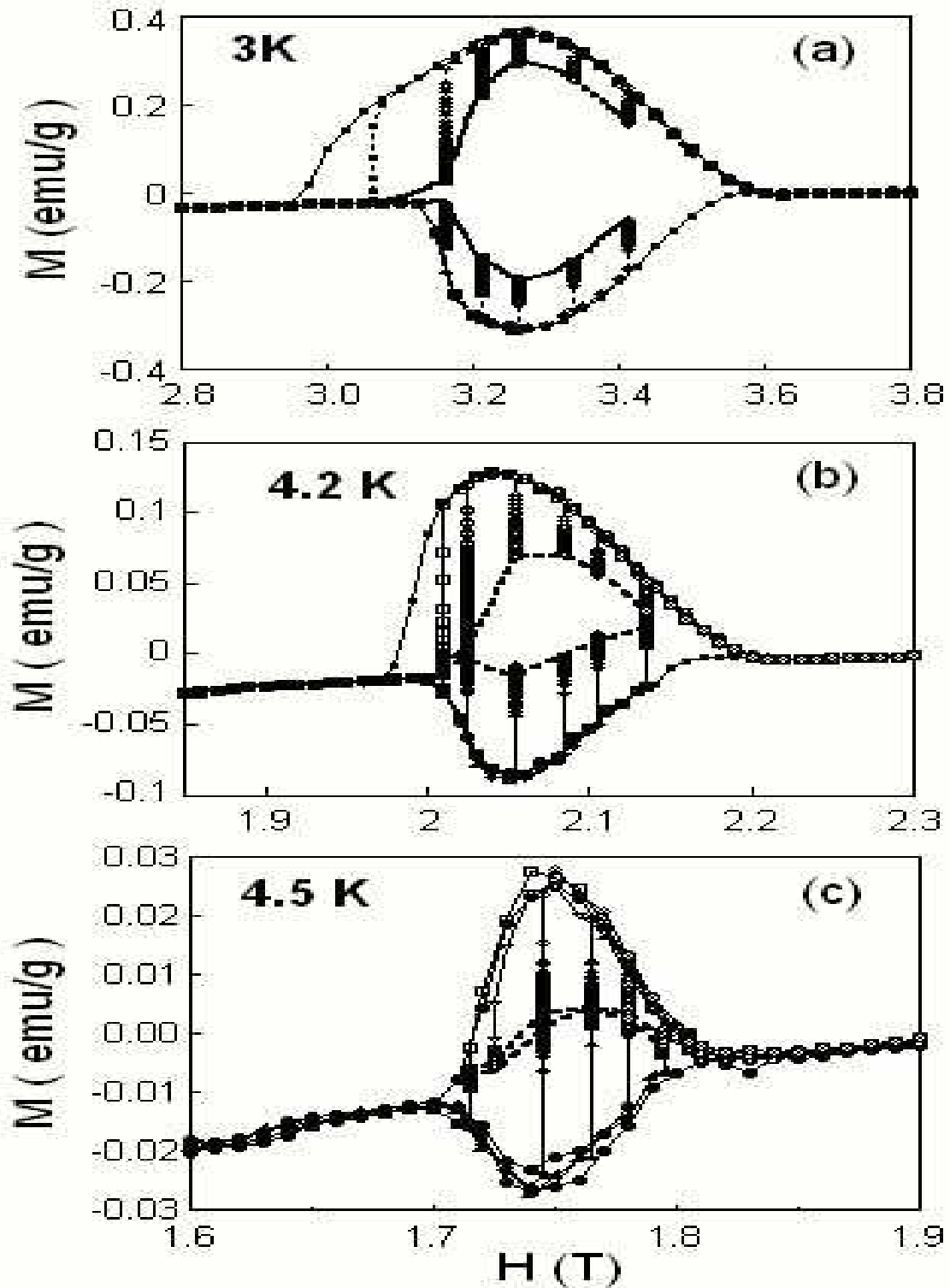


Figure 5: Evolution of the PE hysteresis loops in  $M$  vs  $H$  at 3 K, 4.2 K, and 4.5 K ( $\sim 24$  s between the data points at each  $H$ ). The dotted lines are the connection between the data points at  $\sim 10^4$  s after the initial state. Note the disappearance of the hysteresis loop at 4.5 K.

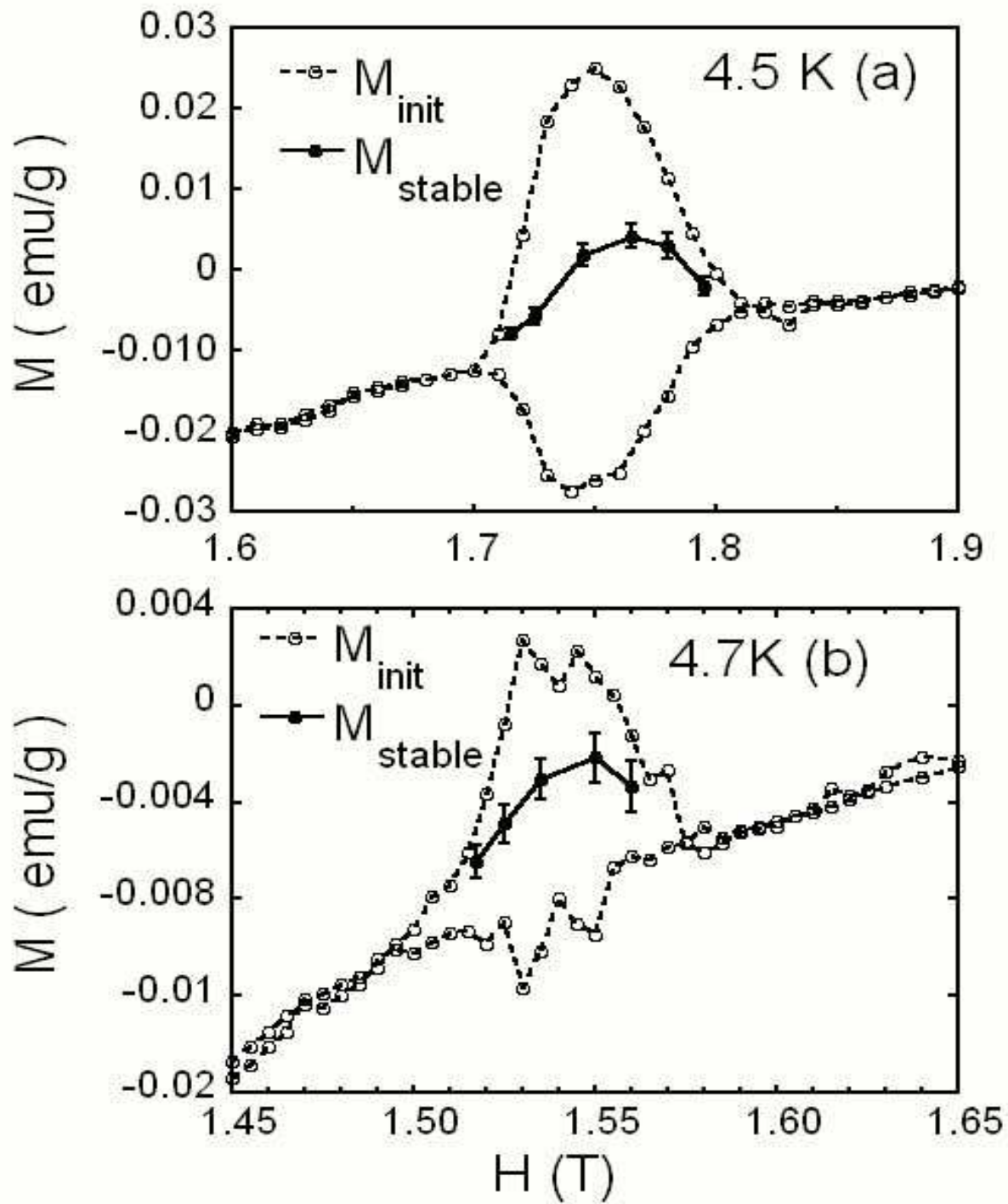


Figure 6: Initial hysteresis loop  $M_{init}(H)$  of the PE and the stable state magnetization ( $M_{stable}(H)$ ) determined from the relaxation data at 4.5 K(a) and 4.7 K(b).

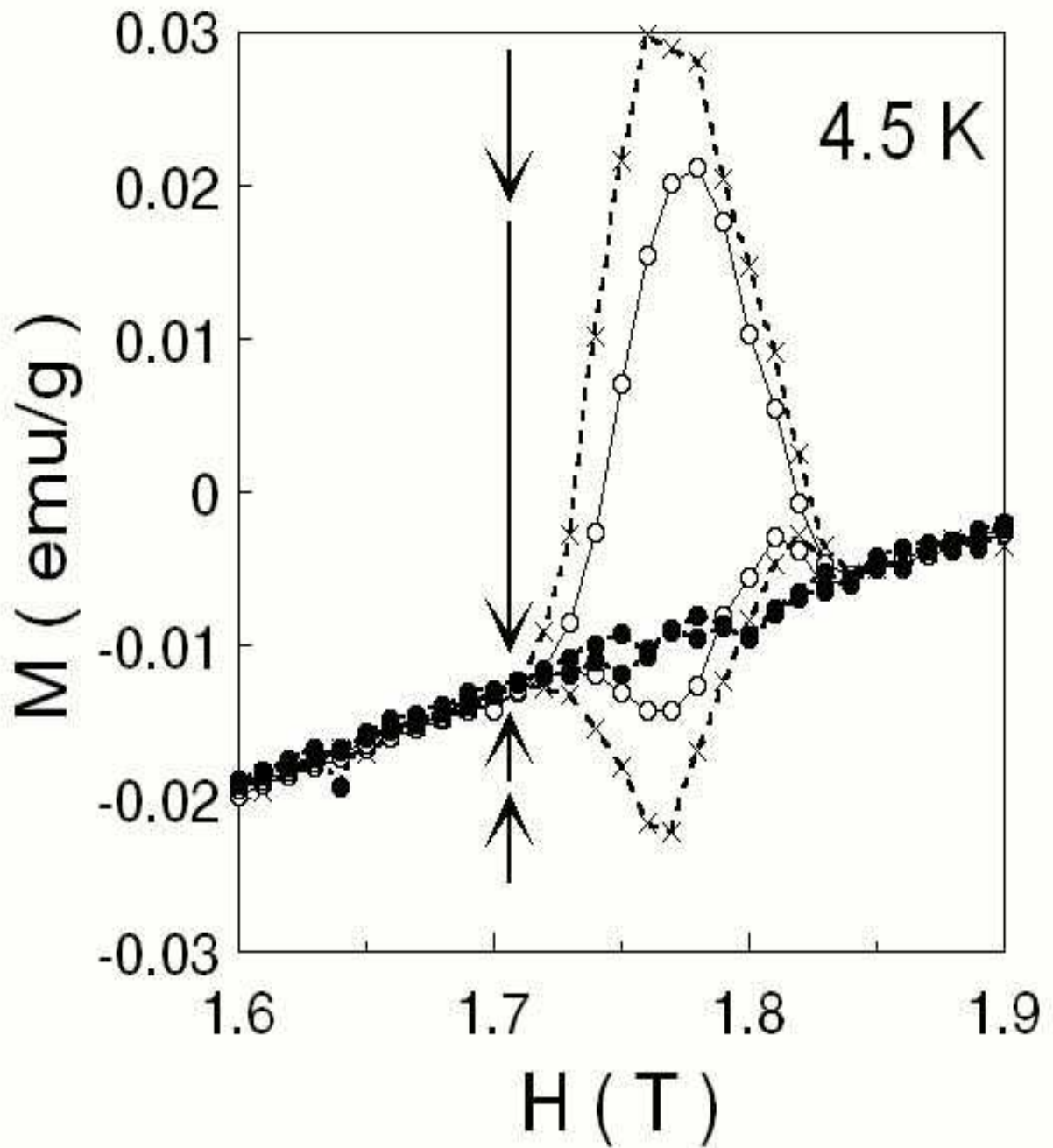


Figure 7: Gradual destruction of the PE hysteresis loops  $M(H)$  at 4.5 K after several rapid thermal cycles between 300 K and 4.5 K. The magnetization ( $\bullet$ ) became reversible and different from the stable state magnetization observed in Fig.6(a).